TELKOMNIKA Telecommunication Computing Electronics and Control
Vol. 24, No. 3, June 2026, pp. 1048~1057
ISSN: 1693-6930, DOI: 10.12928/TELKOMNIKA.v24i3.27620

A study of constrained Bézier fitting curve with tangent continuity for quadruped walking robot gaits

Hung T. Nguyen[1], Minh T. Nguyen[1], Mui D. Nguyen[1], Long Q. Dinh[2], Dung T. Nguyen[2]
[1]Department of Engineering and Technology, Faculty of International Training, Thai Nguyen University of Technology, Thai Nguyen University, Thai Nguyen, Viet Nam
[2]Department of Electronics, Faculty of Engineering and Technology, Thai Nguyen University of Information and Communication Technology, Thai Nguyen, Viet Nam

Article Info

Article history:

Received Oct 20, 2025
Revised Feb 25, 2026
Accepted Mar 29, 2026

Keywords:

Bézier curve
Motion control
MuJoCo simulator
Quadruped robot
Walking gait

ABSTRACT

Smooth and stable gait generation is critical for quadruped robots operating in unstructured environments. This paper introduces a constrained Bézier-fitting framework. It enforces tangent continuity (C^1 continuity) at the gait-cycle junction. This continuity addresses the tangential discontinuities that commonly arise in unconstrained Bézier trajectories. The method formulates foot-trajectory design as a constrained least-squares problem solved via Lagrange multipliers, enabling the control points to simultaneously satisfy interpolation targets and matched-tangent conditions. The resulting curves retain the geometric flexibility of classical Bézier parametrizations while producing well-behaved velocity profiles suitable for legged locomotion. These trajectories are integrated into an impedance-controlled leg model and evaluated in the MuJoCo simulator. Simulation results indicate noticeable reductions in torque spikes and improvements in tracking accuracy when compared to unconstrained Bézier and spline baselines, with representative trials showing reductions on the order of 40% and tracking improvements of approximately 25%. The proposed approach combines mathematical rigor with practical applicability, providing an efficient and reliable solution for high-performance quadruped gait planning.

Corresponding Author:

Minh T. Nguyen
Department of Engineering and Technology, Faculty of International Training
Thai Nguyen University of Technology, Thai Nguyen University
No. 666, 3-2 road, Tich Luong Ward, Thai Nguyen Province, Viet Nam
Email: nguyentuanminh@tnut.edu.vn

1. INTRODUCTION

Quadruped robots have attracted considerable attention for applications in unstructured and dynamic environments, including search and rescue, planetary exploration, and inspection tasks [1]–[3]. Disrupted leg trajectories can destabilize contact with the ground and cause the robot's body to wobble, especially on rough terrain. Therefore, robots need continuous, stable and energy-efficient gaits. They can adapt to a wide variety of terrains and loads. Trajectory planning and motion control are fundamentals to enable stable movement of four-legged robots. Common methods range from zero moment point (ZMP) based planning to optimization techniques and machine learning [4], [5].

Bézier curves are widely used to design foot trajectories because they are simple and easy to control with only a few points. They also ensure smooth and predictable motion since the trajectory always stays inside the region defined by these control points [6]. Many studies use high-degree Bézier curves to describe a full gait cycle with low computation. For example, authors use an 11-point Bézier curve to control the

swing phase, showing good flexibility for both swing and stance motions [7]. Similarly, the authors use Bézier curves for the swing phase in fast trot gaits. They show that Bézier curves give smooth position, velocity and acceleration, and reduce peak leg accelerations compared to cosine-quintic splines [8]. Recent iterative learning control methods use high-order Bézier curves to model periodic gaits like pronking and trotting. This gives smooth joint motions and allows efficient online optimization. Compared to spline methods, Bézier curves are simpler and faster to compute. Spline methods need larger global systems and higher computation [9].

However, ensuring continuity of higher order derivatives at the cycle junction remains a challenge in naive fitting approaches. If the first derivative tangent of the curve at the start and end points fails to match, the resulting trajectory can exhibit jerky transitions and torque spikes, negatively impacting control stability and hardware longevity [10]. This limitation arises because standard Bézier fitting relies on arbitrary or symmetric control-point placement. It does not impose first-derivative constraints at the start-end junction of the gait cycle.

Some methods try to get smooth motion by choosing symmetric control points, but they cannot guarantee perfect tangent continuity. In contrast, this paper adds an explicit constraint to ensure the first derivatives match at the cycle boundary. Previous work uses Bézier curves for gait generation, but they do not strictly enforce tangent continuity. This motivates our constrained least-square Bézier framework. In this paper, we address this gap by proposing a constrained Bézier fitting framework that explicitly enforces C^1 continuity at loop closure. Building on a constrained least squares formulation using Lagrange multipliers, our method derives control points that both interpolate user specified fit points and satisfy a tangential continuity constraint. We integrate the resulting trajectories into an impedance-based leg controller and validate performance in the MuJoCo simulation environment. Comparative experiments against unconstrained Bézier and spline-based trajectories indicate reduced peak acceleration and torque fluctuations, with representative simulations exhibiting improvements on the order of 40% and approximately 25% better tracking accuracy. The proposed approach combines mathematical rigor with practical adaptability, offering a robust solution for high performance quadruped gait planning.

This study introduces a mathematically grounded yet computationally low-complexity approach that improves gait smoothness and stability in simulation. The remainder of this paper is organized as follows. Section 2 provides Bézier curve preliminaries and details the constrained fitting formulation. Section 3 presents simulation results; and finally, section 4 addresses conclusions and future work.

2. GENERATING GAIT PATTERNS USING BÉZIER CURVES

2.1. The Bézier curve

The Bézier curve provides a versatile tool for designing swing-phase trajectories in legged robots, primarily due to its ability to generate a wide variety of smooth curves [11]–[15]. This makes it highly suitable for modeling the natural, fluid motion of a foot during the swing phase, which typically requires both smoothness and precision.

A Bézier curve of degree n, defined by $n+1$ control points $P_0, P_1,\ldots,P_N \in R^3$, is expressed as:

$$B(s)=\sum_{i=0}^{n} P_i \times b_{i,n}(s), \qquad s\in[0,1] \tag{1}$$

where $b_{i,n}(s)$ are the Bernstein basis polynomials given by (2).

$$b_{i,n}(s)=\binom{n}{i}(1-s)^{n-1}s^i \tag{2}$$

The (1) ensures that the resulting curve $B(s)$ is always contained within the convex hull of its control points, leading to intuitive and geometrically predictable behavior. Standard properties of Bernstein polynomials and time-parameter mappings are omitted for brevity and can be found in [16]. Crucially, the trajectory can be modified in a local and smooth manner simply by adjusting the control points P_i. This property allows designers or control algorithms to adapt the swing trajectory in real-time by updating control points according to the parameters output from a gait pattern generator (e.g., step height, duration, or direction). In this paper, we use the same seventh curve fit points ($n = 6$) proposed in [7] shown in (3) and denote $d \in \mathbb{R}$ as the robot step length, $h \in \mathbb{R}$ as the step height and $\theta \in \mathbb{R}$ as the angular variable.

The Bézier curve for steps in space at different orientations, with a step length of $d = 100$ mm and $d = 0$ mm and height of $h = 60$ mm, $P3 = [0, 0.085, 0.3]$ is shown in Figure 1. The Bézier curve uses the points P_0 to P_6 as control points, not necessarily interpolated points. Therefore, the Bézier curve only passes through P_0 and P_6. It approximates the intermediate control points, creating a coherent path influenced by them. The piecewise definition of $u(t)$ follows [7] and is summarized here for completeness as (4).

The (4) maps the physical time $t \in [0, T_p]$ to the Bézier parameter $u \in [0, 1]$ with desired step frequency $f_p = 1/T_p$ duty factor β_t, and internal Bézier duty cycle $\beta_u = 0.6$. This nonlinear mapping ensures that the support phase (middle of the Bézier curve, between P_2 and P_4) aligns with β_t, and the swing phases (both ends) are adjusted to maintain temporal consistency with real-time locomotion.

$$\begin{aligned} d_x &= d \times 0.7 \times \cos(\theta), \\ d_y &= d \times 0.7 \times \sin(\theta), \\ P_0 &= [P_{3x}, P_{3y}, P_{3z} + h], \\ P_1 &= [P_{3x} + d_x \times (4/5), P_{3y} + d_y \times (4/5), P_{3z} + h \times (3/5)], \\ P_2 &= [P_{3x} + d_x, P_{3y} + d_y, P_{3z} + h \times (1/5)], \\ P_3 &= [P_{3x}, P_{3y}, P_{3z}], \\ P_4 &= [P_{3x} - d_x, P_{3y} - d_y, P_{3z} + h \times (1/5)], \\ P_5 &= [P_{3x} - d_x \times (4/5), P_{3y} - d_y \times (4/5), P_{3z} + h \times (3/5)], \\ P_6 &= P_0 \end{aligned} \tag{3}$$

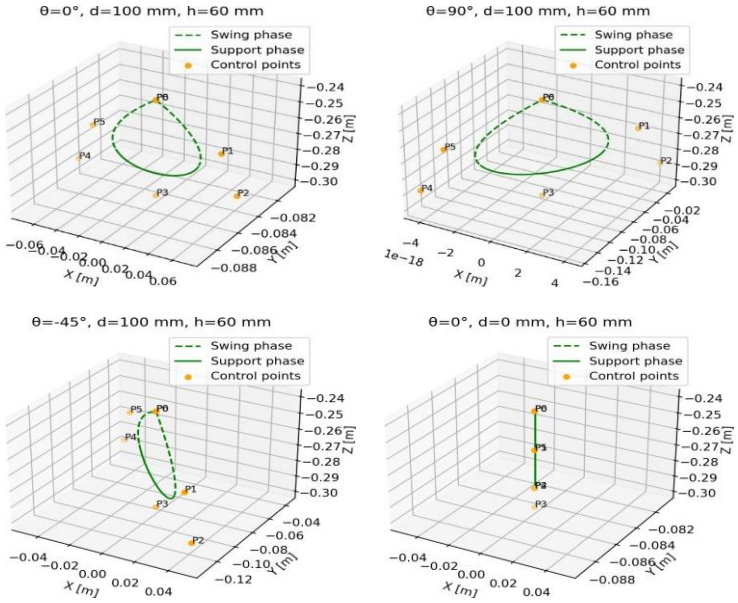

Figure 1. Bézier curves

$$u(t) = \begin{cases} \frac{t}{T_p}\left(\frac{\beta_u - 1}{\beta_t - 1}\right), & 0 \le \frac{t}{T_p} < \frac{1-\beta_t}{2} \\ \frac{\beta_u\left(\frac{2t}{T_p} - 1\right)}{2\beta_t} + 0.5, & \frac{1-\beta_t}{2} \le \frac{t}{T_p} \le \frac{1+\beta_t}{2} \\ \frac{\beta_u}{2} - \frac{(\beta_u - 1)\left(\beta_t - \frac{2t}{T_p} + 1\right)}{2(\beta_t - 1)} + 0.5, & \frac{1+\beta_t}{2} < \frac{t}{T_p} \le 1 \end{cases} \tag{4}$$

2.2. Bézier curve fitting

To guarantee the Bézier curve passes through all control points P_0, to P_6 and forms a coherent closed trajectory, Ebrahimi and Loghmani [17] propose a least-squares fitting method expressed as:

$$W = M^{-1}(T^T T)^{-1} T^T P \tag{5}$$

where $W \in \mathbb{R}^{(n+1)\times m}$ is the matrix of control point weights, with each row W_i representing one control point, $M \in \mathbb{R}^{(n+1)\times(n+1)}$ is a diagonal matrix containing the binomial coefficients derived from the polynomial expansion of the Bézier basis, $P \in \mathbb{R}^{(n+1)\times m}$ is the matrix of target fitting points, where each row corresponds to a point P_i, $T \in \mathbb{R}^{(n+1)\times(n+1)}$ is the temporal matrix, with each row $u_i = [1 \quad u \quad u^2 \quad \cdots \quad u^n]$ constructed

from a time parameter $u \in [0,1]$ assigned to each point P_i. The parameters u_i used to construct the temporal matrix T are obtained by evaluating the mapping in (4) at uniformly sampled phase instants t_i over one gait cycle, corresponding to the interpolation points P_i. In the following discussion, we distinguish between control points, which determine the Bézier curve geometry, and interpolation points, which the curve is constrained to interpolate. This formulation allows for optimal fitting of a Bézier curve to a set of points in a least-squares sense while preserving the geometric structure of the curve. By this fashion, these P_i points are no longer control points, but interpolation targets as shown in Figure 2. As can be seen in Figure 2, even though the Bézier curve now passes through all 7 points P_0 to P_6, the visual discontinuity at the junction $P_0 = P_6$ breaks the C^1 continuity (consistency in velocity) because we enforced the curve to pass through the end points. However, the first derivative at P_0 does not match the derivative at P_6 unless the surrounding control points P_1 and P_5 are suitably chosen.

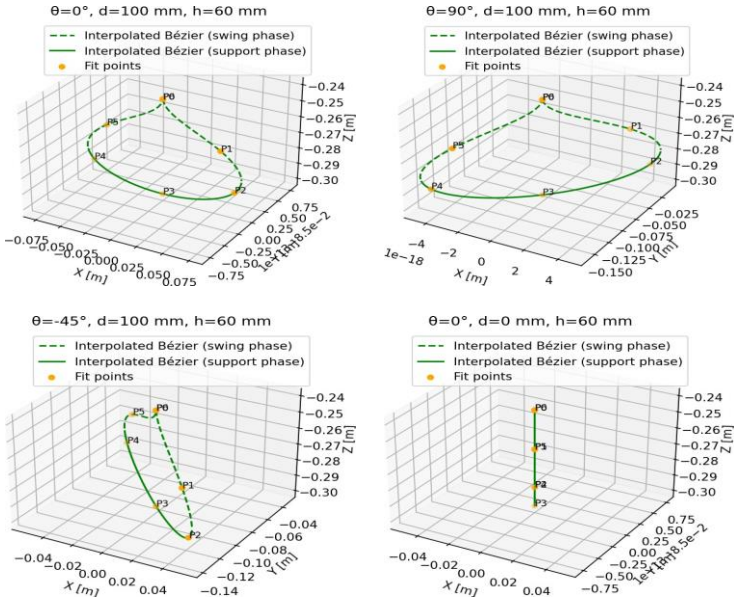

Figure 2. Bézier curve fitted through all points, showing a tangent mismatch at the loop junction

To ensure physically feasible and visually smooth swing trajectories in legged locomotion, tangent continuity must be enforced in Figure 3. The dashed curve is only position-continuous (C^0 continuity) and has a sudden change in direction at the end. This causes discontinuity in velocity. The solid curve enforces tangent continuity (C^1) by aligning the incoming and outgoing tangents. As a result, the velocity is smooth and the motion is more realistic for a robot.

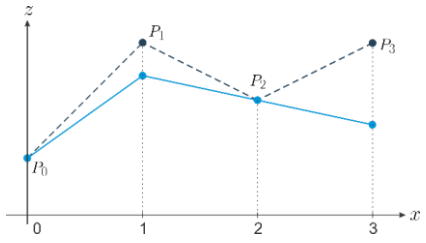

Figure 3. Tangent continuity illustration in a simplified trajectory

A 6th-degree Bézier curve is adopted to remain consistent with prior work [7], as it provides sufficient flexibility to model both swing and stance phases while keeping the number of parameters low. We will fit a 6th-degree Bézier curve through points $P_0, P_1, \ldots, P_6$, enforce interpolation $B(u_i) = P_i$ for $i = 0 \ldots 6$, and add a constraint to enforce tangent continuity at the start/end.

$$W_1 - W_0 = -(W_6 - W_5) \quad (6)$$

The (6) enforces equality of the incoming and outgoing tangent vectors at the loop junction, ensuring that the velocity direction remains continuous across the start-end connection of the gait cycle. This gives us a constrained linear system:

$$AW = P \tag{7}$$

$$CW = 0 \tag{8}$$

where $A \in \mathbb{R}^{7\times7}$ is the Bernstein basis matrix, $W \in \mathbb{R}^{7\times3}$ are control points, and $C \in \mathbb{R}^{1\times7}$ is the constraint matrix. Specifically, the constraint matrix is defined as $C = [-1, 1, 0, 0, 0, 1, -1]$, which directly enforces equality between the incoming and outgoing tangent vectors at the loop junction. The (7) enforces that the fitted Bézier curve passes through all specified interpolation points, while (8) applies the tangent-matching constraint that shapes the curve at the loop junction.

We will solve this using constrained least squares via the method of Lagrange multipliers:

$$\min_{W} \|AW - P\|^2 \text{ subject to } CW = 0 \tag{9}$$

This gives the augmented system (Karush Kuhn Tucker (KKT) conditions). The KKT system couples the fitting objective with the tangent constraint. As a result, the computed control points satisfy both interpolation accuracy and continuous velocity continuity [18], [19].

$$\begin{bmatrix} A^TA & C^T \\ C & 0 \end{bmatrix}\begin{bmatrix} W \\ \lambda \end{bmatrix} = \begin{bmatrix} A^TP \\ 0 \end{bmatrix} \tag{10}$$

where $\lambda \in R^{1\times3}$ is a Lagrange multiplier. The curve with enforced tangent continuity at the connection point $P_0 = P_6$ using a constrained Bézier fitting approach as shown in Figure 4. The constrained system (10) was solved using a standard dense linear solver. Since the matrix size is fixed at 7×7, the computational cost remains negligible ($\mathcal{O}(n^3)$), enabling real-time use in gait generation. Given the small and fixed problem size, the augmented KKT system remains well-conditioned in practice, and no numerical instability was observed in the simulations. As can be seen in Figure 4, the constrained Bézier fitting curve now passes through all 7 points P_0 to P_6 and it is continuous at the loop junction with matched tangents.

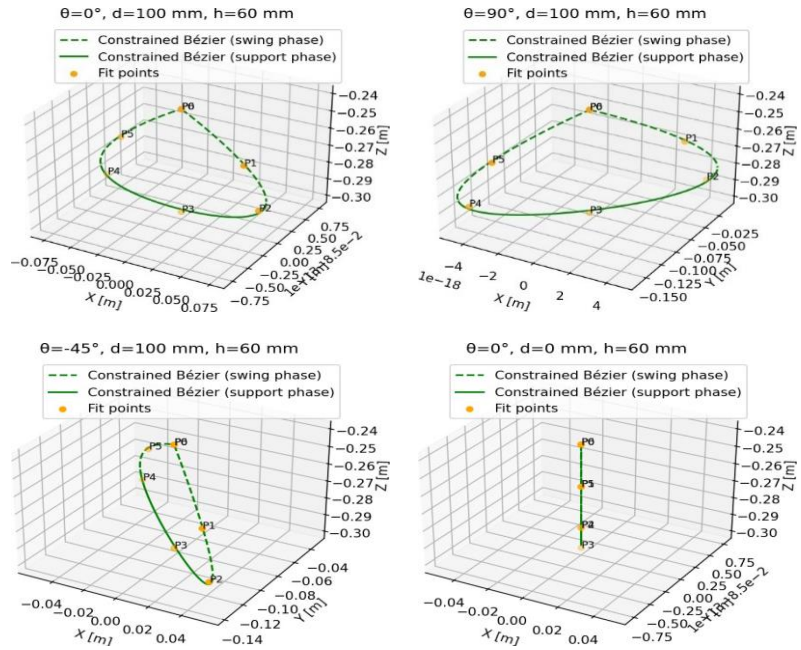

Figure 4. Constrained Bézier curve ensuring tangent continuity at loop closure

3. SIMULATION RESULTS

The Bézier trajectories were integrated into a four-leg impedance controller to generate foot-level force commands. Joint torques were computed using inverse kinematics (IK) followed by Jacobian mapping, and the resulting motions were validated using the MuJoCo physics simulator [20]. After obtaining the Bézier curves for the robot steps, we define the desired foot position $x_d(s)$, the velocity $\dot{x}_d(s)$, the acceleration $\ddot{x}_d(s)$, and an impedance controller that generates the force:

$$F = -K_x(x - x_d) - B_x(\dot{x} - \dot{x}_d) + M_x\ddot{x}_d \tag{11}$$

This force is mapped into joint torques using:

$$\tau = J^T F \tag{12}$$

where J is the Jacobian from joint to foot space as proposed in [7]. This allows us to force each leg of the robot following a Bézier curve trajectory defined in 3D over a normalized gait phase $s \in [0, 1]$. The foot trajectories along a straight path are shown in Figure 5, illustrating alternating swing and stance phases generated by the proposed Bézier framework. The plot depicts the vertical z versus horizontal x motion of each foot over time as the robot walks forward. Each leg follows a parameterized Bézier trajectory in 3D space with a static walking pattern where the legs are phase-shifted as follows: left front (LF) starts at phase 0, right hind (RH) at 0.25, right front (RF) at 0.5, and left hind (LH) at 0.75. The resulting foot paths exhibit alternating swing and stance phases, producing continuous, periodic trajectories. The symmetry and regularity in the patterns reflect consistent and coordinated foot placement, indicative of a stable static gait. Each swing phase is characterized by a curved arc rising in z, followed by a nearly horizontal stance phase at a lower height.

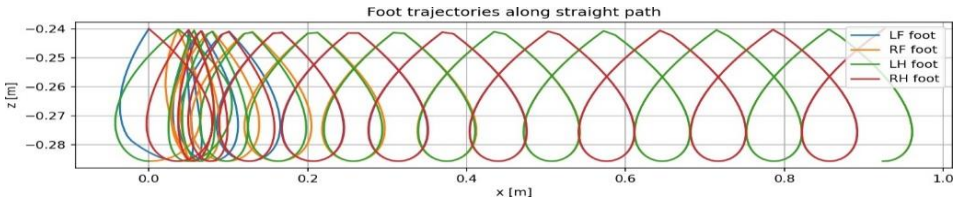

Figure 5. Foot trajectories along a straight path

The MuJoCo simulation setup of the Unitree Go1 robot used to validate the proposed gait generation method is shown in Figure 6.

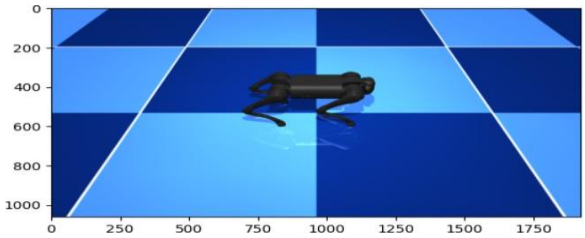

Figure 6. Unitree Go1 Robot simulated in the MuJoCo framework

For each foot trajectory from the Bézier generator, we convert from 3D body frame position to leg-local 2D frame (x, z) and apply IK to compute joint angles. The IK model maps foot position (x, z) to joint angles θ_1, θ_2, θ_3 using (13)-(15):

$$\theta_2 = \cos^{-1}\left(\frac{x^2+z^2-l_2^2-l_3^2}{2l_2l_3}\right) \tag{13}$$

$$\theta_1 = \tan^{-1}\left(\frac{z}{x}\right) - \tan^{-1}\left(\frac{l_3 \sin(\theta_2)}{l_2 + l_3 \cos(\theta_2)}\right) \quad (14)$$

$$\theta_0 = \text{base orientation compensation or hip offset} \quad (15)$$

with the length from hip to thigh link $l_1 = 0.213$ m, and the length from thigh to calf link $l_2 = 0.213$ m. After that we stack all 4 legs into 12 joint positions, differentiate over time to get joint velocities, and produce a gait data file with 24 rows (rows 0-11 are joint positions (abduction, thigh, calf for 4 legs, rows 12-23 are joint velocities computed via finite difference) and 100 times steps for 1 gait cycle at 100 Hz. We apply the model-predictive path integral control and the Python code for the MuJoCo simulation given in [21] to test the movement of the Unitree Go1. The simulation results show that the robot legs follow the trajectories of the Bézier curves as in Figure 7.

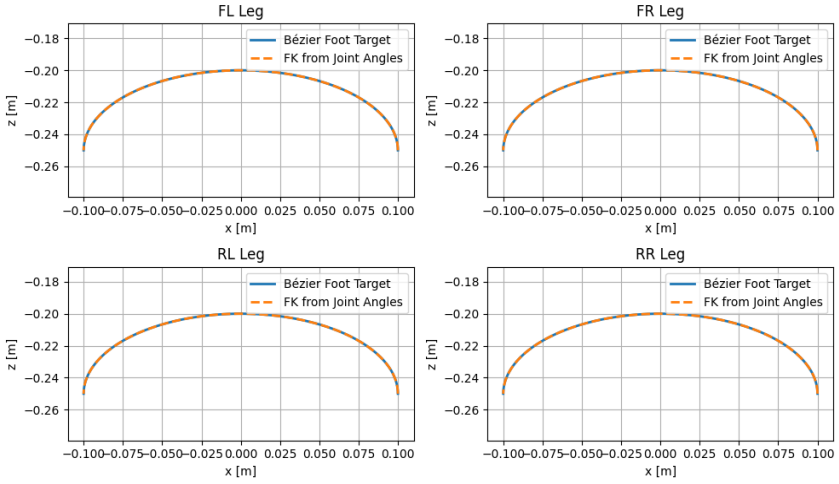

Figure 7. Comparison between reference Bézier trajectories and forward-kinematics (FK) reconstruction from joint angles for 4 legs

In Figure 7, the reconstructed trajectories obtained via FK (dashed lines) closely match the reference Bézier trajectories (solid lines), indicating accurate tracking for all four legs and validating the effectiveness of the IK and trajectory generation. The observed improvements in trajectory smoothness and loop continuity are consistent with prior studies on constrained parametric gait representations for legged robots. Enforcing first-derivative continuity has been shown to reduce impact forces and improve control stability in cyclic locomotion patterns [22], [23]. Compared to spline-based gait optimization methods that rely on global continuity constraints [24], the proposed constrained Bézier formulation maintains local geometric flexibility while preserving computational efficiency. Simulation-based validation using high-fidelity physics engines has been widely adopted in recent legged-robot research to evaluate gait generation and control strategies prior to hardware deployment. Large-scale simulation studies have shown that accurate modeling of contact dynamics and actuator behavior can provide reliable insight into locomotion performance on real quadruped platforms. In this context, the MuJoCo-based evaluation employed in this work offers a credible and commonly accepted benchmark for assessing the effectiveness of constrained trajectory generation methods [25].

4. CONCLUSION

This paper introduced a constrained Bézier-fitting framework that enforces tangent continuity at the gait-cycle junction, effectively eliminating velocity discontinuities that typically cause jerky foot motions and torque spikes. By formulating the fitting process as a constrained least-squares problem with Lagrange multipliers, the method computes control points that both interpolate the designer-specified foot placements and satisfy a first-derivative matching constraint. When integrated into an impedance-based leg controller and evaluated in MuJoCo, the resulting trajectories were tracked with high fidelity, and reconstruction through FK nearly overlapped the original Bézier curves. Comparative experiments indicate notable reductions in peak accelerations and torque fluctuations, with representative simulation runs showing

improvements on the order of 40% and approximately 25% gains in tracking accuracy, translating into smoother and more robust locomotion with reduced mechanical stress. It should be noted that these percentage improvements are indicative and based on representative simulation runs rather than a comprehensive statistical evaluation.

Future work will explore physical validation on quadruped platforms, extension of the method to enforce C^2 continuity for improved jerk minimization, and integration with adaptive or reinforcement-learning controllers capable of adjusting control points in response to terrain variation or proprioceptive feedback. We will also investigate the sensitivity of the constrained fitting formulation to perturbations in interpolation points.

ACKNOWLEDGMENTS

The authors would like to thank Thai Nguyen University of Technology (TNUT), Viet Nam.

FUNDING INFORMATION

Authors state there is no external funding involved.

AUTHOR CONTRIBUTIONS STATEMENT

This journal uses the Contributor Roles Taxonomy (CRediT) to recognize individual author contributions, reduce authorship disputes, and facilitate collaboration.

Name of Author	C	M	So	Va	Fo	I	R	D	O	E	Vi	Su	P	Fu
Hung T. Nguyen	✓				✓			✓	✓	✓			✓	
Minh T. Nguyen		✓		✓		✓			✓	✓		✓		✓
Mui D. Nguyen	✓								✓					
Long Q. Dinh			✓		✓		✓		✓					
Dung T. Nguyen	✓			✓				✓	✓	✓				

C : **C**onceptualization
M : **M**ethodology
So : **So**ftware
Va : **Va**lidation
Fo : **Fo**rmal analysis
I : **I**nvestigation
R : **R**esources
D : **D**ata Curation
O : Writing - **O**riginal Draft
E : Writing - Review & **E**diting
Vi : **Vi**sualization
Su : **Su**pervision
P : **P**roject administration
Fu : **Fu**nding acquisition

CONFLICT OF INTEREST STATEMENT

Authors state no conflict of interest.

DATA AVAILABILITY

The data that support the findings of this study are available from the corresponding author upon request.

REFERENCES

[1] Q. Li, F. Cicirelli, A. Vinci, A. Guerrieri, W. Qi, and G. Fortino, "Quadruped Robots: Bridging Mechanical Design, Control, and Applications," *Robotics*, vol. 14, no. 5, p. 57, Apr. 2025, doi: 10.3390/robotics14050057.

[2] Z. Zhou, Z. Chen, M. Cai, Z. Li, Z. Kan, and C. Y. Su, "Vision-Based Reactive Temporal Logic Motion Planning for Quadruped Robots in Unstructured Dynamic Environments," *IEEE Transactions on Industrial Electronics*, vol. 71, no. 6, pp. 5983–5992, Jun. 2024, doi: 10.1109/TIE.2023.3299048.

[3] A. Hamrani, M. M. Rayhan, T. Mackenson, D. McDaniel, and L. Lagos, "Smart quadruped robotics: a systematic review of design, control, sensing and perception," *Advanced Robotics*, vol. 39, no. 1, pp. 3–29, Jan. 2025, doi: 10.1080/01691864.2024.2411684.

[4] S. Dong, F. Fan, Y. Chen, S. Guo, and J. Liu, "Gait Planning, and Motion Control Methods for Quadruped Robots: Achieving High Environmental Adaptability: A Review," *CMES - Computer Modeling in Engineering and Sciences*, vol. 143, no. 1, pp. 1–50, 2025, doi: 10.32604/cmes.2025.062113.

[5] Y. Fan, Z. Pei, C. Wang, M. Li, Z. Tang, and Q. Liu, "A Review of Quadruped Robots: Structure, Control, and Autonomous Motion," *Advanced Intelligent Systems*, vol. 6, no. 6, Jun. 2024, doi: 10.1002/aisy.202300783.

[6] J. Delgado and J. M. Peña, "Geometric properties and algorithms for rational q-Bézier curves and surfaces," *Mathematics*, vol. 8, no. 4, p. 541, Apr. 2020, doi: 10.3390/math8040541.

[7] G. D. G. Pedro *et al.*, "Quadruped Robot Control: An Approach Using Body Planar Motion Control, Legs Impedance Control and

Bézier Curves," *Sensors*, vol. 24, no. 12, p. 3825, Jun. 2024, doi: 10.3390/s24123825.
[8] X. Zeng, S. Zhang, H. Zhang, X. Li, H. Zhou, and Y. Fu, "Leg trajectory planning for quadruped robots with high-speed trot gait," *Applied Sciences (Switzerland)*, vol. 9, no. 7, p. 1508, Apr. 2019, doi: 10.3390/APP9071508.
[9] J. Cheng, Y. G. Alqaham, Z. Gan, and A. K. Sanyal, "Iteratively Learning Muscle Memory for Legged Robots to Master Adaptive and High Precision Locomotion," *arXiv*, Apr. 2026, doi: 10.48550/ARXIV.2507.13662.
[10] M. Chen, K. Zhang, S. Wang, F. Liu, J. Liu, and Y. Zhang, "Analysis and Optimization of Interpolation Points for Quadruped Robots Joint Trajectory," *Complexity*, vol. 2020, pp. 1–17, Jul. 2020, doi: 10.1155/2020/3507679.
[11] N. T. Nguyen, P. T. Gangavarapu, N. F. Kompe, G. Schildbach, and F. Ernst, "Navigation with Polytopes: A Toolbox for Optimal Path Planning with Polytope Maps and B-spline Curves," *Sensors*, vol. 23, no. 7, p. 3532, Mar. 2023, doi: 10.3390/s23073532.
[12] M. Benko Loknar, G. Klančar, and S. Blažič, "Minimum-Time Trajectory Generation for Wheeled Mobile Systems Using Bézier Curves with Constraints on Velocity, Acceleration and Jerk," *Sensors*, vol. 23, no. 4, p. 1982, Feb. 2023, doi: 10.3390/s23041982.
[13] Y. L. Kuo, C. C. Lin, and Z. T. Lin, "Dual-optimization trajectory planning based on parametric curves for a robot manipulator," *International Journal of Advanced Robotic Systems*, vol. 17, no. 3, May 2020, doi: 10.1177/1729881420920046.
[14] S. Zhang, Q. Hou, X. Zhang, X. Wu, and H. Wang, "A Novel Vectorized Curved Road Representation Based Aerial Guided Unmanned Vehicle Trajectory Planning," *Sensors*, vol. 23, no. 16, p. 7305, Aug. 2023, doi: 10.3390/s23167305.
[15] B. Jin *et al.*, "Joint Torque Estimation toward Dynamic and Compliant Control for Gear-Driven Torque Sensorless Quadruped Robot," in *IEEE International Conference on Intelligent Robots and Systems*, IEEE, Nov. 2019, pp. 4630–4637, doi: 10.1109/IROS40897.2019.8968168.
[16] V. Bulut, "The optimal path of robot end effector based on hierarchical clustering and Bézier curve with three shape parameters," *Robotica*, vol. 40, no. 9, pp. 3266–3289, Sep. 2022, doi: 10.1017/S0263574722000182.
[17] A. Ebrahimi and G. B. Loghmani, "B-spline Curve Fitting by Diagonal Approximation BFGS Methods," *Iranian Journal of Science and Technology, Transaction A: Science*, vol. 43, no. 3, pp. 947–958, Jun. 2019, doi: 10.1007/s40995-017-0347-1.
[18] A. Agrawal, R. Verschueren, S. Diamond, and S. Boyd, "A rewriting system for convex optimization problems," *Journal of Control and Decision*, vol. 5, no. 1, pp. 42–60, Jan. 2018, doi: 10.1080/23307706.2017.1397554.
[19] G. Giorgi, B. Jiménez, and V. Novo, "Approximate Karush–Kuhn–Tucker Condition in Multiobjective Optimization," *Journal of Optimization Theory and Applications*, vol. 171, no. 1, pp. 70–89, Oct. 2016, doi: 10.1007/s10957-016-0986-y.
[20] K. Zakka *et al.*, "MuJoCo Playground," Feb. 2025, [Online]. Available: http://arxiv.org/abs/2502.08844
[21] J. Alvarez-Padilla, J. Z. Zhang, S. Kwok, J. M. Dolan, and Z. Manchester, "Real-Time Whole-Body Control of Legged Robots with Model-Predictive Path Integral Control," *Proceedings - IEEE International Conference on Robotics and Automation*, pp. 14721–14727, Sep. 2025, doi: 10.1109/ICRA55743.2025.11128271.
[22] M. Hutter *et al.*, "ANYmal - A highly mobile and dynamic quadrupedal robot," in *IEEE International Conference on Intelligent Robots and Systems*, IEEE, Oct. 2016, pp. 38–44, doi: 10.1109/IROS.2016.7758092.
[23] P. Fankhauser, M. Bjelonic, C. D. Bellicoso, T. Miki, and M. Hutter, "Robust Rough-Terrain Locomotion with a Quadrupedal Robot," in *Proceedings - IEEE International Conference on Robotics and Automation*, IEEE, May 2018, pp. 5761–5768, doi: 10.1109/ICRA.2018.8460731.
[24] C. Mastalli, I. Havoutis, M. Focchi, D. G. Caldwell, and C. Semini, "Motion planning for quadrupedal locomotion: Coupled planning, terrain mapping, and whole-body control," *IEEE Transactions on Robotics*, vol. 36, no. 6, pp. 1635–1648, Dec. 2020, doi: 10.1109/TRO.2020.3003464.
[25] J. Hwangbo *et al.*, "Learning agile and dynamic motor skills for legged robots," *Science Robotics*, vol. 4, no. 26, Jan. 2019, doi: 10.1126/scirobotics.aau5872.

BIOGRAPHIES OF AUTHORS

Hung T. Nguyen is currently working as a lecturer at the Department of Electrical Engineering, Faculty of International Training, Thai Nguyen University of Technology - Thai Nguyen University. His main research interests include topics in robust control, linear parameter varying control of nonlinear systems, gain-scheduling design, and their applications in electric drive systems. He can be contacted at email: h.nguyentien@tnut.edu.vn.

Minh T. Nguyen is currently the director of human resource training and development center at Thai Nguyen University, Vietnam, and also the director of advanced wireless communication networks (AWCN) lab. He has interest and expertise in a variety of research topics in the communications, networking, and signal processing areas, especially compressive sensing, and wireless/mobile sensor networks. He serves as technical reviewers for several prestigious journals and international conferences. He also serves as an editor for wireless communication and mobile computing journal and an editor in chief for ICSES transactions on computer networks and communications. He can be contacted at email: nguyentuanminh@tnut.edu.vn.

Mui D. Nguyen is currently working as a lecturer at the Department of Electrical Engineering, Faculty of International Training, Thai Nguyen university of Technology - Thai Nguyen University. He graduated from university with a major in Electronics and Telecommunications in 2015 and completed his Master's degree in Electronic Engineering in 2018. Currently, he is pursuing a Ph.D. in Control and Automation Engineering at the same university where he has been attached for many years. He is a member of the advanced wireless communication networks (AWCN) laboratory. He can be contacted at email: ducmui@tnut.edu.vn.

Long Q. Dinh is currently working as a lecturer at the Department of Engineering and Technology, Thai Nguyen University of Information and Communication Technology (ICTU) - Thai Nguyen University. He graduated with a Bachelor's degree in Automation in 2011 from Hanoi University of Science and Technology and completed his Master's degree in Control and Automation in 2015 from the same university. He is a member of the advanced wireless communication networks (AWCN) laboratory. His main research interests include intelligent control. He can be contacted at email: dqlong@ictu.edu.vn.

Dung T. Nguyen is a lecturer at the Faculty of Engineering and Technology, Information and Communication Technology University (ICTU), Vietnam. He graduated with a Bachelor's degree in Electronics and Telecommunications Engineering from ICTU in 2011 and completed his Master's degree in Biomedical Engineering from Hanoi University of Science and Technology (HUST) in 2014. He is a member of the advanced wireless communication networks (AWCN) laboratory. His main research interests include intelligent control and wireless sensors. He can be contacted at email: ntdungcndt@ictu.edu.vn.